

Electron-beam induced crystallization transition in self-developing amorphous AlF_3 resists

G. S. Chen

Department of Materials Science, Feng Chia University, Taichung 407, Taiwan

C. B. Boothroyd and C. J. Humphreys

Department of Materials Science and Metallurgy, University of Cambridge, Cambridge CB2 3QZ, United Kingdom

(Received 21 February 1996; accepted for publication 30 April 1996)

Transmission electron microscopy is used to investigate electron-induced crystallization of thermally evaporated amorphous AlF_3 ($a\text{-AlF}_3$). It is shown that this material undergoes a very complicated crystallization process with three crystalline substances (Al , AlF_3 , and Al_2O_3) formed as the dose increases. The sequence of the crystallization is highly sensitive to the presence of water, which inhibits radiolytic dissociation of $a\text{-AlF}_3$ into Al and fluorine, reduces the dose required for the crystallization of $a\text{-AlF}_3$, and causes the transformation of AlF_3 into Al_2O_3 . © 1996 American Institute of Physics. [S0003-6951(96)01128-X]

Direct electron beam writing on low-molecular weight, ionic oxides, and halide materials is currently the most promising method for defining ultra-small nanostructures.¹ Such materials have potential applications as high-resolution electron beam resists, or for high density information storage. Among which amorphous aluminum trifluoride ($a\text{-AlF}_3$) is almost the most attractive material being used as a positive or negative self-developing resist.^{2,3} Several research groups have demonstrated the potential of the subnanometer cutting and ruling by an intense beam of electrons (SCRIBE) "hole-drilling" technique because well-defined nanometer-scale holes and lines can be cut through about 50 nm of $a\text{-AlF}_3$ in only about a few milliseconds.⁴⁻⁷ However, because $a\text{-AlF}_3$ is so sensitive to beam irradiation, its exposure mechanism is still not fully understood and contradictory results have even been presented.^{6,7} In addition, that water can play a role during the SCRIBE/hole drilling process has been widely suspected, but its effects in modifying the drilling mechanisms have rarely been quantitatively studied.^{8,9} We have noted that previous researchers always assume that the exposure behavior of $a\text{-AlF}_3$ is unaffected by the humidity of the films. However, $a\text{-AlF}_3$ films are normally porous and contain varying amounts of water, some of which is chemically bonded to the AlF_3 and some of which is absorbed on the surface and in the pores.¹⁰ We have first demonstrated that $a\text{-AlF}_3$ films undergo a series of very complicated crystallization transition processes, which are highly sensitive to the presence of water, if irradiated in conventional transmission electron microscopes (TEMs).¹¹ In this letter, we use electron microscopy to present a means of semiquantitatively analyzing the effect of the water on the crystallization process of this material.

The crystallization process was investigated with a JEOL 2000FX TEM operating at an accelerating voltage of 100 kV in conjunction with a Gatan parallel electron energy loss spectrometer (EELS). All films (50 nm) were deposited with an Edwards 306 thermal evaporator onto carbon supporting films (~5 nm) on standard TEM grids. The deposition rate, monitored with a quartz thickness monitor, was 0.4 nm/s.

Figure 1 shows a dark field image, recorded from the $a\text{-AlF}_3$ diffuse ring (inset) and with minimum dose, which exhibits speckle contrast characteristic of amorphous materials. A diffraction pattern from a briefly damaged $a\text{-AlF}_3$ film is shown in Fig. 2 (inset). It can be seen that the $a\text{-AlF}_3$ undergoes a crystallization transition upon irradiation forming Al and crystalline AlF_3 ($c\text{-AlF}_3$). After prolonged irradiation a strong 0.14 nm diffraction ring of Al_2O_3 also emerges. Dark field images of the irradiated crystalline products (Al and AlF_3) are shown in Fig. 2 from which it can be seen that the Al microcrystallites are randomly oriented, while the $c\text{-AlF}_3$ has more variable grain sizes. Selected area diffraction instead of imaging technique was performed to investigate the process of the crystallization transition since the films were so sensitive to beam damage that it was difficult to record a few images without causing serious damage.

In order to assess the effect of water on the crystallization of $a\text{-AlF}_3$, we studied two types of thermally evaporated films. For the dry films, anhydrous AlF_3 was heated at 400 °C for 10 h to remove water prior to evaporation. For the wet films, $\text{AlF}_3 \cdot 3\text{H}_2\text{O}$ was evaporated without preheating. Evaporation of the dry films was carried out at a pressure of

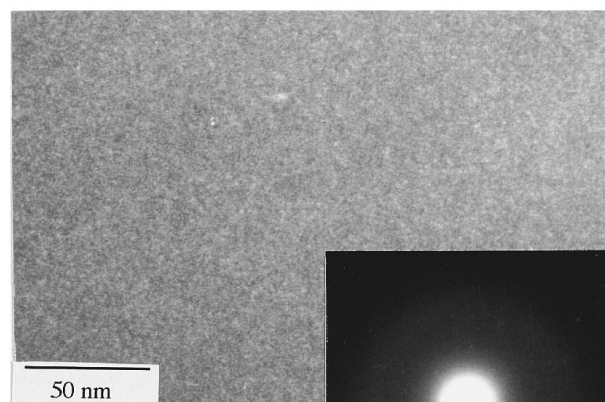


FIG. 1. Dark field image taken using an aperture on the AlF_3 diffuse ring (inset) showing the amorphous structure of the as-prepared evaporated AlF_3 .

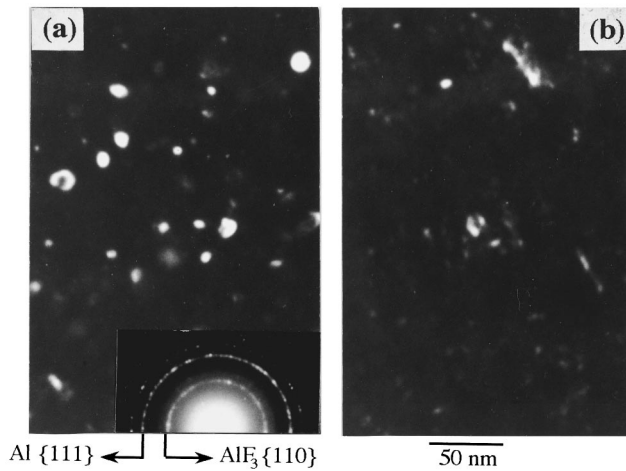


FIG. 2. Diffraction pattern (inset) showing the Al{111} and AlF₃{110} rings. (a) and (b) show dark field images taken from the same region of an irradiated AlF₃ film using objective apertures on the Al{111} and AlF₃{110} rings, respectively.

$\sim 5 \times 10^{-6}$ mbars whereas the wet films were evaporated at a much higher pressure ($\sim 1 \times 10^{-4}$ mbars) caused by the release of the hydrated water. The amount of water left in the films was identified using transmission infrared spectroscopy, which showed that the wet films had an enormous absorption band at $3 \mu\text{m}$ (O–H stretch) while this absorption band in the dry films was negligible. Infrared spectroscopy also showed that the AlF₃ films absorbed water rapidly when they were exposed to air. X-ray diffractometer showed that all types of heated powder possessed the same (tetragonal) structure. All the films were freshly prepared and transferred to the TEM within 15 min of preparation. The beam current was measured with a Faraday cage at the side of the specimens, which was routinely checked every ~ 10 min, making sure that any decay of beam current was compensated for. The same area of the specimen was irradiated throughout each experiment, with the irradiation being stopped at frequent intervals for a series of diffraction patterns to be obtained. Diffraction patterns from each series were then digitized and radially averaged to produce electron intensity as a function of scattering angle. Figure 3 shows typical resultant

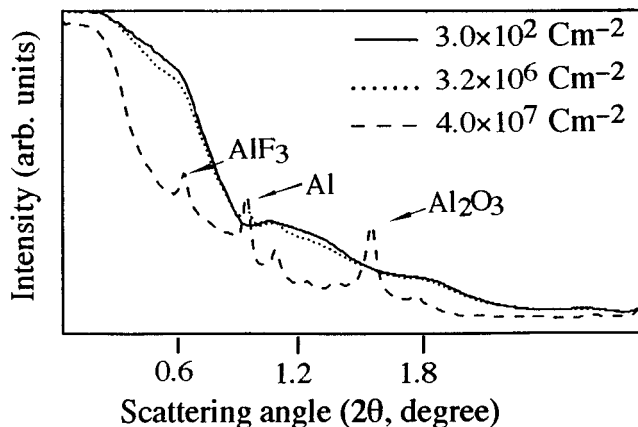


FIG. 3. Radial average of diffraction patterns from a series showing the progress of crystallization transition from Al, to AlF₃, then Al₂O₃.

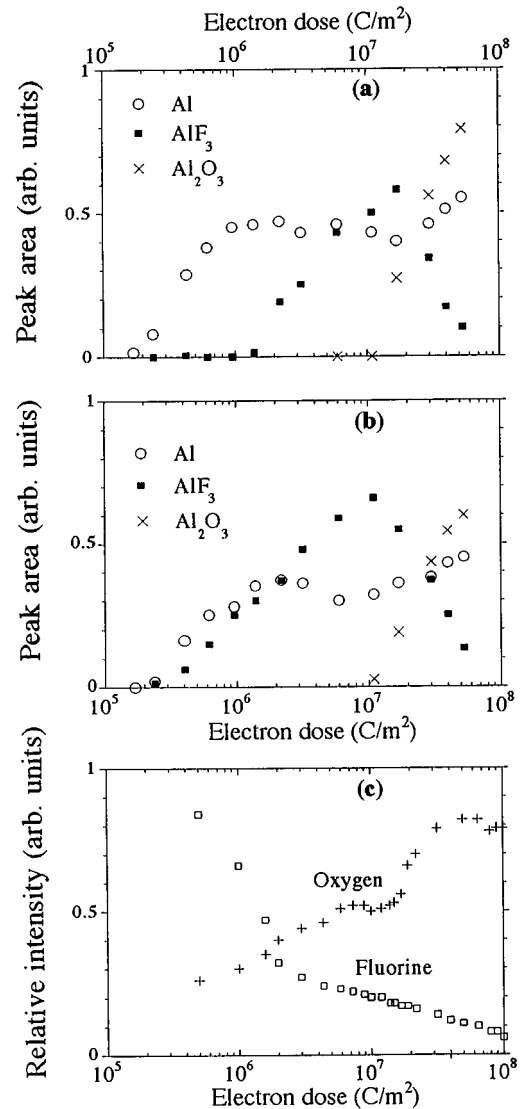


FIG. 4. Normalized diffraction peak areas of the Al{111}, *c*-AlF₃{110}, and the Al₂O₃ 0.14 nm ring as a function of dose for (a) dry and (b) wet types of films. All patterns were taken under identical conditions, therefore, the peak areas are comparable between the two figures. It is to be noted that the total amount of AlF₃ in the film cannot be directly judged from the *c*-AlF₃ {110} peak area because this sharp peak is on top of a very broad diffuse peak of *a*-AlF₃. (c) shows the integrated counts of the O 535 eV and F 685 eV K edges (measured within a 50 eV window) as a function of dose.

diffraction intensities of three diffraction patterns from a series for the dry type of films irradiated at a current density of $6.9 \times 10^3 \text{ A m}^{-2}$, showing that the damage process is gradual with the broad peaks of *a*-AlF₃ disappearing and sharp peaks of crystalline substances appearing.

For each of the two types of films, diffraction patterns were obtained (strictly under identical conditions to each other) over a range of doses from 10^5 to 10^8 C m^{-2} . The diffraction patterns were radially averaged as in Fig. 3 and the areas under the most prominent peak for each crystalline reaction product found. Figures 4(a) and 4(b) plot the diffraction peak areas as a function of dose for the two types of films, allowing the crystallization process to be monitored as a function of dose. The crystallization behavior of Al for the two types of films at low dose regime is similar. However, a

much lower dose ($\sim 2 \times 10^5 \text{ C m}^{-2}$) is needed for the $a\text{-AlF}_3$ to crystallize in the wet films than in the dry films ($\sim 1 \times 10^6 \text{ C m}^{-2}$). In addition, if the dry films are exposed to air for a few days then their behaviors become more like those of the wet films. For a dry AlF_3 film, measurements were made of the areas under the oxygen and fluorine EELS K edges as a function of dose [Fig. 4(c)]. It can be seen that up to a dose of $1 \times 10^6 \text{ C m}^{-2}$, fluorine decreases rapidly, then more slowly and at a uniform rate above this dose. $1 \times 10^6 \text{ C m}^{-2}$ corresponds to the dose when $a\text{-AlF}_3$ starts to crystallize. Thus, up to $1 \times 10^6 \text{ C m}^{-2}$, fluorine is being lost and the AlF_3 remains amorphous. At $1 \times 10^6 \text{ C m}^{-2}$, the $a\text{-AlF}_3$ begins to crystallize and is more stable to damage, so the rate of loss of fluorine decreases.

Al_2O_3 crystallites are observed in the two types of films at high dose regime. Figures 4(a) and 4(b) show that, over the range of doses from 8×10^6 to $5 \times 10^7 \text{ C m}^{-2}$, where the Al_2O_3 is visible, the rapid increase of the Al_2O_3 signal is consistent with the fast decrease of the $c\text{-AlF}_3$ signal, but the intensity of Al declines only slightly. Energy loss spectra reveal that the oxygen 535 eV K edge is present in all as-prepared films and increases a little during irradiation at low doses, even though no crystalline Al_2O_3 is observed at these doses. The oxygen (presumably water picked up from the microscope vacuum, $\sim 1 \times 10^6$ mbars) is incorporated into the films as the fluorine is lost. Above $1 \times 10^7 \text{ C m}^{-2}$, Al_2O_3 suddenly begins to form, corresponding to an abrupt increase in the oxygen signal at this dose and a sudden decay in the $c\text{-AlF}_3$. Above $5 \times 10^7 \text{ C m}^{-2}$, the concentration of oxygen levels off when all the $c\text{-AlF}_3$ has reacted, and the Al_2O_3 itself may be decomposing due to irradiation.¹² We have also noted that, in some (electron-beam deposited) $a\text{-AlF}_3$ films, the intensity of Al was very weak within doses from $\sim 1 \times 10^6$ to $5 \times 10^7 \text{ C m}^{-2}$, but the signals of $c\text{-AlF}_3$ and Al_2O_3 were similar to those of Figs. 4(a) and 4(b). The intensity of the Al_2O_3 kept increasing even though there was no detectable Al left after the dose exceeded $\sim 1 \times 10^7 \text{ C m}^{-2}$.¹³ As the Al is almost negligible, it is thus unlikely that the Al_2O_3 is directly transformed from reactions of the Al with any compound. From the above results, we believe that the Al_2O_3 is transformed from reaction of (amorphous and crystalline) AlF_3 with an oxygen-related compound (presumably water), and therefore propose a possible chemical reaction mechanism: $2\text{AlF}_3 + 3\text{H}_2\text{O} \rightarrow \text{Al}_2\text{O}_3 + 6\text{HF}$.

Previous investigations into the possibility of using thermally evaporated AlF_3 as an optical film have shown that its structure is porous with a packing density of $\sim 60\%$ of bulk AlF_3 and water can be easily incorporated into the film.^{14,15} This study has found that the "wet" AlF_3 is prone to crystallization at the low dose regime and $c\text{-AlF}_3$ is formed to-

gether with Al colloids as a result of beam irradiation. This could have a significant effect on the hole-drilling behavior of this material. It is known that the crystallinity of a material plays a crucial role in deciding the transport properties of species produced during hole-drilling.¹⁶⁻¹⁸ For $a\text{-AlF}_3$, an abundance of data have already confirmed that it is a "popping" type of drilling material, which exhibits an abrupt mass-loss behavior and tends to be associated with displacement of dissociated produce (Al) from irradiated volume and anion aggregation to form bubbles of fluorine gas. It requires a threshold dose of $\geq 10^5 \text{ C m}^{-2}$ for the bubbles to "pop." For the wet films, the dose required to begin to form Al is approximately the same as that for which crystallization of the remaining $a\text{-AlF}_3$ occurs, and is about the same magnitude as the threshold dose for hole drilling. As $c\text{-AlF}_3$ is more resistant to radiolysis than $a\text{-AlF}_3$, and given the dependence of hole drilling on the structure (crystalline or amorphous) of a material already discussed by many researchers, clearly the transition of $a\text{-AlF}_3$ to $c\text{-AlF}_3$ will alter the subsequent hole-drilling behavior of AlF_3 and thus retard the drilling process.

In summary, we have shown that the electron-beam damage of dry $a\text{-AlF}_3$ is a very complicated process, whereby crystalline Al is formed first as fluorine is lost, followed by the crystallization of $a\text{-AlF}_3$ and the formation of Al_2O_3 . It is important to note that the water content of the films can greatly alter the doses required for each substrate to crystallize.

- ¹C. J. Humphreys, T. J. Bullough, R. W. Devenish, and D. M. Maher, *Inst. Phys. Conf. Ser.* **119**, 319 (1991).
- ²A. Murray, M. Scheinfein, and M. Isaacson, *J. Vac. Sci. Technol. B* **3**, 367 (1985).
- ³E. Kratschmer and M. Isaacson, *J. Vac. Sci. Technol. B* **5**, 369 (1987).
- ⁴C. A. Walsh, *Philos. Mag. A* **59**, 227 (1989).
- ⁵Y. Ito, A. L. Bleloch, S. J. R. Granleese, and L. M. Brown, *Inst. Phys. Conf. Ser.* **138**, 507 (1993).
- ⁶R. M. Allen, S. J. Lloyd, and C. J. Humphreys, *Inst. Phys. Conf. Ser.* **138**, 87 (1993).
- ⁷V. I. Nikolaichik, *Philos. Mag. A* **68**, 227 (1993).
- ⁸P. M. Mankiewich, H. G. Craighead, T. R. Harrison, and A. H. Dayem, *Appl. Phys. Lett.* **44**, 468 (1984).
- ⁹R. W. Devenish, D. J. Eaglesham, D. M. Maher, and C. J. Humphreys, *Ultramicroscopy* **28**, 324 (1989).
- ¹⁰J. D. Targove, B. G. Bovard, L. J. Lingg, and H. A. Macleod, *Thin Solid Films* **159**, L57 (1988).
- ¹¹G. S. Chen, C. B. Boothroyd, and C. J. Humphreys, *Inst. Phys. Conf. Ser.* **119**, 325 (1991).
- ¹²C. J. Morgan, S. J. Bailey, A. R. Preston, and C. J. Humphreys, *Inst. Phys. Conf. Ser.* **119**, 503 (1991).
- ¹³G. S. Chen, Ph.D. thesis, University of Cambridge, 1994.
- ¹⁴W. Heitmann, *Thin Solid Films* **5**, 6 (1970).
- ¹⁵A. P. Bradford, G. Hass, and M. McFarland, *Appl. Opt.* **11**, 2242 (1972).
- ¹⁶R. M. Allen, Ph.D. thesis, University of Cambridge, 1992.
- ¹⁷R. Zanetti, A. L. Bleloch, M. Grimshaw, J. H. Paterson, and G. A. C. Jones, *Inst. Phys. Conf. Ser.* **138**, 67 (1993).
- ¹⁸C. J. Morgan, Ph.D. thesis, University of Cambridge, 1994.